

Blocking SHH/Patched interaction triggers tumor growth inhibition through Patched-induced apoptosis

Pierre-Antoine Bissey^{1,\$}, Pauline Mathot¹, Catherine Guix¹, Mélissa Jasmin¹, Isabelle Goddard^{1,2}, Clélia Costechareyre¹, Nicolas Gadot³, Jean-Guy Delcros¹, Sachitanand M. Mali⁴, Rudi Fasan⁴, André-Patrick Arrigo¹, Robert Dante¹, Gabriel Ichim⁵, Patrick Mehlen^{1,3#} and Joanna Fombonne^{1#}

¹Apoptosis, Cancer and Development Laboratory- Equipe labellisée 'La Ligue', LabEx DEVweCAN, Cancer Research Center of Lyon (CRCL), INSERM U1052-CNRS UMR5286, Université de Lyon, Centre Léon Bérard, Lyon, France

²Department of Translational Research and Innovation, Centre Leon Bérard, Laboratoire des Modèles Tumoraux (LMT) Fondation Synergie Lyon Cancer

³Department of Translational Research and Innovation, Anapath, Centre Léon Bérard, Lyon

⁴Department of Chemistry, University of Rochester, Rochester, NY, USA

⁵Cancer Cell death Lab, Cancer Research Center of Lyon (CRCL), Université de Lyon, Centre Léon Bérard, Lyon, France

Co-senior authors

^{\$}Present address: Princess Margaret Cancer Center- University Health Network, Toronto, Ontario, Canada

RUNNING TITLE:

Activation of Patched-induced apoptosis slows tumor growth

CORRESPONDING AUTHORS:

Patrick Mehlen, University of Lyon-CRCL, Centre Léon Bérard, 28 rue Laennec, Lyon 69008, France. Phone: 334-7878-2870; Fax: 334-7878-2887; E-mail: patrick.mehlen@lyon.unicancer.fr

Joanna Fombonne, University of Lyon-CRCL, Centre Léon Bérard, 28 rue Laennec, Lyon 69008, France. Phone: 334 7878 5972, Fax: 334-7878-2887; E-mail: joanna.fombonne@lyon.unicancer.fr

CONFLICTS OF INTEREST:

The authors declare no potential conflicts of interest

KEYWORDS:

Patched-1, Hedgehog signaling, dependence receptor, cell death, therapeutic target

ABSTRACT:

The Sonic Hedgehog (SHH) pathway plays a key role in cancer. Alterations of SHH canonical signaling, causally linked to tumor progression, have become rational targets for cancer therapy. However, Smoothed (Smo) inhibitors have failed to show clinical benefit in patients with cancers displaying SHH autocrine/paracrine expression. We reported earlier that the SHH receptor Patched (Ptc) is a dependence receptor that triggers apoptosis in the absence of SHH through a pathway that differs from the canonical one, thus generating a state of dependence on SHH for survival. Here, we propose a dual function for SHH: its binding to Ptc not only activates the SHH canonical pathway but also blocks Ptc-induced apoptosis. 80%, 64% and 8% of human colon, pancreatic and lung cancer cells, respectively, overexpressed SHH at transcriptional and protein levels. In addition, SHH-overexpressing cells expressed all the effectors of the Ptc-induced apoptotic pathway. While the canonical pathway remained unchanged, autocrine SHH interference in colon, pancreatic and lung cell lines triggered cell death through Ptc pro-apoptotic signaling. In vivo, SHH interference in colon cancer cell lines decreased primary tumor growth and metastasis. Therefore, the anti-tumor effect associated to SHH deprivation, usually thought to be a consequence of the inactivation of the canonical SHH pathway, is due to the engagement of Ptc pro-apoptotic activity. Together, these data strongly suggest that therapeutic strategies based on the disruption of SHH/Ptc interaction in SHH-overexpressing cancers should be explored.

STATEMENT OF SIGNIFICANCE:

Sonic Hedgehog-overexpressing tumors express Ptc-induced cell death effectors, suggesting that this signaling could be activated as an anti-tumor strategy.

INTRODUCTION

The morphogen Sonic Hedgehog (SHH) regulates many developmental processes including ventrodorsal patterning of the neural tube, establishment of limb polarity and development of the foregut and axio-cranial skeleton (1,2). SHH signaling is mainly mediated *via* the binding of SHH to the twelve-transmembrane receptor Patched 1 (Ptc) which relieves Ptc suppressive effect towards Smoothed (Smo), an orphan seven-transmembrane receptor, that initiates a signaling cascade leading to the activation of the glioma-associated (Gli) transcription factors.

In adults, SHH signaling is mainly quiescent, being physiologically reactivated only during tissue maintenance and repair (3). However, during tumor formation and progression, deregulation of SHH signaling has been reported to often occur and be detrimental (for review, (4)),(5-8). Indeed, many different types of human cancers display abnormal activation of SHH signaling (4)(9-11), promoting this pathway as a choice target for the development of new therapeutics. So far, two types of strategies to antagonize the “canonical” SHH-Ptc-Smo-Gli signaling pathway have been worked out. The first strategy was to design Smo- or Gli-antagonists that target the active signaling pathway. In clinical trials, even though some resistance and important side effects were reported, some of these hedgehog pathway inhibitors, such as the Smo antagonist Vismodegib or Sonidegib, showed good anti-tumor activity in tumors bearing genetic alterations of the "canonical pathway", such as Basal Cell Carcinoma (BCC) and medulloblastoma, (for review, (12)). However, in tumors characterized by an up-regulation of SHH clinical trials were far less efficient. The second strategy was aimed to target the upstream initiation of the SHH pathway. Indeed, a large fraction of human

cancer displays SHH up-regulation (4,11)) that can be neutralized either by targeting SHH production –e.g., oligonucleotides targeting SHH gene- or by blocking SHH interaction with Ptc –e.g., blocking monoclonal antibody (13,14). Despite several reports describing the inhibition of tumor growth and the induction of tumor cell apoptosis in various animal models using monoclonal antibodies targeting SHH (15,16), this approach never reached patient clinical trial level.

These therapeutic strategies were all designed according to the classic view that Ptc is a basic receptor that is solely active when bound to SHH. However, we recently demonstrated that Ptc has the fascinating property to also be able to trigger cell apoptosis in the absence of its ligand. Ptc is thus a dependence receptor (17). More recently, another SHH receptor, CDON (Cell-adhesion molecule-related/down-regulated by Oncogenes) has also been described as a dependence receptor able to trigger cell death in absence of SHH (18). Such receptors are two-sided receptors: while they induce a positive signal (promoting cell survival, migration, proliferation) in the presence of their ligand, they can induce an active process of apoptotic cell death in the absence of ligand. These dependence receptors include p75^{ntr}, DCC (Deleted in Colorectal Cancer), UNC5H, Neogenin, Notch3 and the RET, EPHA4, Alk and c-Kit tyrosine kinase receptors (19-24). The pro-apoptotic activity of dependence receptors is believed to be important not only during embryonic development (17,20,25-27) but also for inhibiting tumor progression. Indeed, the dependence on ligand presence is also thought to act as a safeguard mechanism to prevent tumor cells from developing in settings of ligand unavailability (for reviews, (28,29)). Thus, a tumor cell losing the pro-apoptotic activity of a dependence receptor would gain a selective advantage for growth. Along this line, we

showed that the inactivation of DCC pro-apoptotic signaling in mice is associated with colorectal tumor progression (30). One way to silence this death pathway is to up-regulate the ligand level in the tumor environment –i.e. autocrine or paracrine expression (31-34). Such an up-regulation of SHH is known to occur in a large fraction of human cancers (11, 13,14). Moreover, as CDON is frequently lost in several cancer types (18), we thus hypothesized that the anti-tumor effect observed upon SHH interference is not only due to the inactivation of the SHH signaling canonical pathway but also to the activation of Ptc pro-apoptotic activity involving the recruitment of the caspase activating complex dependosome (35).

In this study, we report that SHH-overexpressing tumors express Ptc-induced cell death effectors suggesting that this signaling could be activated as an anti-tumor strategy. Moreover, we demonstrated in a colon cell line model that blocking SHH triggers Ptc-induced apoptosis through the recruitment of the dependosome complex. Lastly, we provide *in vivo* evidences that the strategy based on interference with SHH/Ptc interaction limits tumor growth through Ptc-induced cell death. Thus, we propose to consider an alternative therapeutic approach where, in SHH-overexpressing resistant tumors, a SHH blocking antibody could show therapeutic benefit.

MATERIALS AND METHODS:

Database analysis

The Cancer Genome Atlas (TCGA) data were downloaded, assembled and processed using TCGA2STAT (36). Subsequent analyses were performed with the R statistical software v 3.3.1 and GraphPad Prism software.

Cell lines and Transfection Procedures

All cell lines were obtained from American Type Culture Collection (ATCC). The human colon cancer cell lines HCT8 and SW1417 were cultured in RPMI 1640 Glutamax medium (Gibco ; Life Technologies) containing respectively 10% horse serum or 10 % FBS. The human colon cell line LoVo, the pancreatic cell line Mia PaCa-2 and the NSCLC cell line A549 were cultured in DMEM Glutamax medium (Gibco ; Life Technologies) containing 10% FBS. The human pancreatic cell line Capan-2 was cultured in RPMI 1640 Glutamax medium (Gibco ; Life Technologies) containing 15% FBS. The mouse fibroblast cell line NIH3T3 was cultured in DMEM Glutamax medium (Gibco ; Life Technologies) containing 10% FBS. All media were supplemented with 1% peni-streptomycin and 0,4% fungizone. Routine Mycoplasma testing was performed by MycoAlert Mycoplasma Detection Kit (catalog no. LT07-118). Cells grown for no more than 20 passages were used in all the experiments. Cell lines were transfected using Lipofectamine Plus Reagent (Life Technologies) for plasmids or Lipofectamine 2000 reagent or RNAi Max (Life Technologies) for small interfering RNA (siRNA).

Plasmid Constructs, siRNA and SHH-neutralizing 5E1 antibody production

The pRK5-Ptc, pRK5-PtcDN-HA (Ptc7IC D1392N), pcDNA3-wild-type caspase-9-3XFLAG, pcDNA3-DRAL-3xFLAGM2 were described earlier (17,35). Stable HCT8 and LoVo cell line expressing PtcDN was established using peak8 vector (clontech) and selected with puromycin (1 µg/ml-Sigma). More precisely, peak8-PtcDN plasmid was obtained by inserting a HindIII/EcoRV fragment generated by polymerase chain reaction

performed on the already described pcDNA3-PtcDN (17). HCT8 and LoVo cells were then transfected with an empty plasmid (peak8 vector) or peak8-PtcDN and was treated with puromycin 48h after transfection. SHH and Control siRNA were designed by Santa Cruz as a pool of three target-specific siRNAs of 20-25 nucleotides. SHH-neutralizing 5E1 monoclonal antibody was purified from ascites on protein G sepharose columns (Biotem). Centricon (Millipore) were used for antibody concentration and buffer exchange. Murine IgG1 isotype control was purchased from R&D System. HL2m5 macrocyclic peptide inhibitor were described in (37).

Immunohistochemistry on human tumors samples

Human pancreatic, colon and Lung cancer Tissues Microarray were obtained from Biochain (Z7020110; T8235722; P3235152). After deparaffinization and dehydration, 4- μ m thick tissue sections were heated for 50 min at 97 °C in citrate buffer pH9. To block endogenous peroxidases, tissue sections were incubated in 5% hydrogen peroxide solution. Immunohistochemistry was performed on an automated immunostainer (Ventana Discovery XT, Roche, Meylan, France) using Omnimap DAB Kit according to the manufacturer's instructions. Sections were incubated with an anti-SHH monoclonal rabbit antibody (Abcam) (diluted at 1:10000), an anti-Ptc polyclonal rabbit (Novus Bio - diluted at 1:500), an anti-DRAL polyclonal rabbit (Abcam - diluted at 1:200) and an anti-Caspase-9 monoclonal mouse (Abcam - diluted at 1:200) were used. Anti-rabbit or Mouse - HRP were applied on sections. Staining was visualized with DAB solution with 3,3'-diaminobenzidine as a chromogenic substrate. Finally, the sections were

counterstained with Gill's hematoxylin then were scanned with panoramic scan II (3D Histech, Budapest, Hungary) at 1x or 2x.

Immunoblotting analysis

Immunoblots were performed as described in (35) using anti-SHH (Abcam), anti-FHL2/DRAL (Abcam), anti-Caspase-9 (Cell signaling), anti-Ptc (Abcam), anti-Ptc C-ter (to detect PtcDN; generously given by M. Ruat and Novus Bio), anti-CDO (Santa Cruz), anti- β actin (Millipore), anti-FLAG (Sigma) and anti-HA (Sigma) antibodies.

Quantitative Reverse Transcription-Polymerase Chain Reaction

To assay SHH, Ptc and CDO expression, total RNA was extracted from cell lines using the NucleoSpin RNAII kit (Macherey Nagel) and 1 μ g was reverse transcribed using the iScript cDNA Synthesis kit (Bio-Rad Laboratories). Real-time Q-RT-PCR was performed as previously described (38). The ubiquitously expressed human β actin was used as an internal control.

Cell death assays

For caspase-3 assays, $1.5 \cdot 10^5$ cells were cultured in serum-free medium and were treated (or not) with SHH-neutralizing 5E1 antibody (5 μ g/mL) for 24h or transfected with 10nM Control, SHH, Ptc or CDO siRNA (Santa cruz) with Lipofectamine 2000 or RNAi Max (Life Technology) for 48h. Apoptosis was monitored by measuring caspase-3 activity using the caspase-3/CPP32 Fluorometric Assay Kit (Gentaure Biovision, Brussels, Belgium) as described previously (38).

For propidium iodide (PI) incorporation, $5 \cdot 10^4$ cells were cultured without serum in the presence of 0,3 ug/ml of propidium iodide and were transfected with 10nM Control, SHH, Ptc or CDO siRNA (Santa cruz) with Lipofectamine 2000 (Invitrogen). Live counting of PI positive cells was done for 72h with the Incucyte Zoom Live cells analysis system (Essen Bioscience) and indexed on percentage of cell confluency.

Chicken model for tumor progression and dissemination

Colon cancer HCT8 cells (10^7 cells) in 20 μ l of PBS were mixed with 20 μ l of Matrigel (BD Bioscience) to form a gel and implanted on top of the CAM of 10-day-old chick embryos. 10 μ g of the control IgG or the 5E1 antibodies were injected in the tumor on days 11 and 13. On day 17, tumors were resected. Primary tumor size and metastasis in lungs were determined as previously described (32). Briefly, on day 17, tumor areas were measured with AxioVision Release 4.6 software (Carl Zeiss, Inc.). To assess metastasis, lungs were harvested from the tumor-bearing embryos and genomic DNA was extracted with a NucleoSpin Tissue kit (Macherey- Nagel). Metastasis was quantified by PCR-based detection of the human Alu sequence (32) using the primers 5'-ACGCCTGTAATCCCAGCACTT-3' (sense) and 5'-TCGCCCAGGCTGGAGTGCA-3'(antisense) with chick GAPDH- specific primers (accession number: M11213.1) (sense, 5'-GAGGAAAGGTCGCCTGGTGGATCG-3'; anti-sense, 5'-GGTGAGGACAAGCAGTGAGGAACG-3') as controls. For both couples of primers, PCR was performed at 95°C for 2 min followed by 30 cycles at 95°C for 30 s, 63°C for 30 s, and 72°C for 30 s. Genomic DNA extracted from lungs of healthy chick embryos was used to determine the threshold between colon cell-invaded and –non-invaded

lungs. To monitor apoptosis in primary tumors, primary tumors and surrounding CAM were resected, and caspase-3 activity was measured on tumor protein lysates using the caspase 3/CPP32 Fluorimetric Assay kit.

Zebrafish metastasis model

Prior to injection, HCT8 peak and PtcDN cells were treated for 48h with IgG isotype control or 5E1 antibodies. Then, 9×10^5 cells were resuspended in serum-free medium and stained with lipophilic dyes DiO or DiD for 20 minutes at 37°C (ThermoFisher). Cells were then washed and resuspended in 30 μ L of PBS. For zebrafish xenotransplantation, 48 hours post-fecundation (hpf) zebrafish embryos were anaesthetized with tricaine (Sigma-Aldrich) and 20 nL of cell suspension (approximately 300 labeled human cells) were injected into the perivitelline cavity of each embryo. The embryos were then placed at 30°C for 24 hours and allowed to recover in the presence of N-phenylthiourea (Sigma-Aldrich) to inhibit melanocyte formation. For imaging and metastasis assessment, zebrafish embryos were anaesthetized with tricaine and imaged using an Axio Observer Zeiss microscope (Zeiss).

Xenograft of human cell lines in nude mice

Five-week-old female Swiss nu/nu mice (20 – 22 g) were obtained from Charles River. Animals were maintained in the specific pathogen free (SPF) animal facility (AniCan) at the Cancer Research Center of Lyon (CRCL) at the Center Léon Bérard. All the experiments were performed in accordance with the animal care guidelines of the European Union and were validated by the local Animal Ethic Evaluation Committee (CECCAPP: C2EA-15 agreed by the French Ministry of High School and Research).

HCT8 Control or PtcDN HCT8 or LoVo cells were implanted by subcutaneous injection of $2 \cdot 10^6$ or $4 \cdot 10^6$ cells, respectively, in 50 μ l of PBS mixed with 50 μ l of Matrigel into the right flank of the mice. When tumors reached a volume of approximately 70 mm³ (around 10 days after injection), 300 μ g of SHH neutralizing 5E1 antibody or an equal volume of buffer was injected 3 times per week for maximum 23 days. In other experiments, 3 μ g of siRNA targeting SHH or control siRNA was injected intraperitoneally 3 times per week for 9 days. Tumor sizes were measured with a caliper. The tumor volume was calculated with the formula $v = 0.5 (l \times w \times w)$, where v is volume, l is length, and w is width. To monitor apoptosis, tumors were resected and broken up in a lysis buffer from the caspase 3/ CPP32 Fluorimetric Assay kit and caspase-3 activity was measured in tumor protein lysates.

Statistical analysis

The statistical significance of differences between groups was evaluated by the paired Student t test or the Mann–Whitney test, two-way ANOVA test for tumor volume mice comparison and Chi-squared test for the comparison of lung metastasis percentage in chick embryo models.

Mean values for all outcome variables are presented with 95% confidence intervals. Data presented are representative of at least three independent experiments. All statistical tests were two-sided, and results were considered significant at $p < 0.05$.

RESULTS

SHH-overexpressing tumors express the Ptc-proapoptotic signaling repertoire

Previous studies have reported that a high proportion of colon and pancreatic cancers overexpress SHH (8,39). This was confirmed by analyzing TCGA relative SHH expression in a large panel of tumor samples (colon cancer n = 283, pancreatic cancer n = 178 and lung cancer n = 1016). We found respectively that 80%, 64% and 8% of colon, pancreatic and lung cancers overexpress SHH when compared to normal tissues (two times more than the average SHH mRNA level in normal tissues) (Fig 1A, B). Of note, while SHH is not correlated to patient survival rate in colon or in pancreatic cancers (Suppl Fig 1A, B), it is interesting to point out that in pancreatic cancer, SHH expression is significantly increased according to the advanced stages (Suppl Fig 1C, D). The overexpression of SHH at transcriptional level is corroborated by SHH immunohistochemistry analyses on colon, pancreatic and lung tumoral tissues, showing especially a strong epithelial staining of SHH in the 76,7% and 57,3% of colon and pancreatic tumor samples, respectively (60 colon and 89 pancreatic tumor samples were analyzed) (Fig 1C and Suppl Fig 1E, F). Moreover, most of colon and pancreatic tumors showing overexpression of SHH show a very high score of SHH expression (score 2 and 3) (Suppl Fig 1G).

Further analysis indicated that SHH-overexpressing tumors also highly express Ptc as well as Ptc-mediated death effectors, – i.e. the caspase activating complex leading to Ptc-induced cell death (35). Indeed, as seen in Figure 1D, the genes encoding PTCH1, caspase-9, FHL2, CARD8/NLRP1 and NEDD4 were notably expressed in SHH-overexpressing tumors, which is confirmed at protein level by immunohistochemistry on human colon and pancreatic cancer tissues for Ptc protein (Fig 1C) and for FHL2 and

Caspase-9 (Suppl Fig 1H, I), suggesting that they bear a putative functional Ptc-proapoptotic signaling.

Interfering with SHH triggers Ptc-apoptotic cell death

We then investigated whether in SHH-expressing tumor cells, SHH is constitutively inhibiting Ptc-induced apoptosis by SHH. To do so, we selected representative human tumor cell lines of colon cancers (HCT8, SW1417, LoVo), pancreatic cancers (Mia PaCa-2, Capan-2) and NSCLC (A549) based on their expression of SHH, Ptc and the main Ptc-mediated known death effector, i.e. FHL-2 and caspase-9 (35). As seen in Figure 2A and Suppl Fig 2A), the levels of Ptc and caspase-9 expression analyzed by immunoblot were similar in all selected cell lines whereas SHH and FHL2 expression level was variable.

We then analyzed cell death in response to the disruption of SHH autocrine loop. As a first approach, SHH was down-regulated by RNA interference. As shown in Figure 2B and Suppl Fig 2B, the transient transfection of SHH small interfering RNA (siRNA SHH) was associated with a significant reduction in SHH mRNA in all cell lines studied. The down-regulation was confirmed at protein level in HCT8 cells (Suppl Fig 2C). This reduction was accompanied with an activation of caspase-3 in all cell lines (Fig. 2C and Suppl Fig 2D), used as a read-out for dependence receptor-induced cell death assessment. Of high interest, we were also able to show increase cell death in HCT8 cells upon SHH interference using a macrocyclic peptide HL2m5 (37) able to abolish SHH/Ptc interaction (Suppl Fig 2E). To decipher the mechanisms involved in this response, we then focused on the colorectal cancer HCT8 cells then we confirmed the

results in colorectal cancer LoVo cells. We first confirmed in HCT8 cells the causal relationship between SHH silencing effect and caspase-3 activation: treatment with exogenous recombinant SHH (rSHH) prevented caspase-3 activation in SHH silenced cells (Fig. 2D). Caspase-3 activation was associated with increased PI staining supporting the view that caspase activation lead to cell death (Fig 2E and Suppl Fig 3A, B). Moreover, the siRNA-mediated down-regulation of Ptc (Fig 2F) fully inhibited SHH siRNA-mediated cell death (Fig 2E and Suppl Fig 3A, B), hence demonstrating that the cell death observed upon SHH silencing is mediated by Ptc. Given that we previously reported that CDON receptor also triggers apoptosis when unbound to its ligand SHH (18), we analyzed the level of CDON expression by immunoblot in HCT8 cell line. While the RH30 rhabdomyosarcoma cell line used as a positive control expressed a high amount of CDON protein, we failed to detect CDON expression in HCT8 (Suppl Fig 3C). Given that CDON expression was detected at mRNA level, we performed cell death assay upon CDON silencing by siRNA in HCT8 (Suppl Fig 3D). Down-regulation of CDON failed to inhibit SHH silencing-induced cell death (Suppl Fig 3A, E, F). Taken together these results suggest that the cell death induced by SHH down-regulation in HCT8 cells is specifically mediated by Ptc receptor.

In order to confirm that the death induction described above results from Ptc pro-apoptotic activity, we generated HCT8 and LoVo stably expressing a mutant of Ptc –i.e., Ptc-71C-D1392N- (PtcDN) that was reported to act as a specific dominant negative mutant for Ptc pro-apoptotic activity (Fig 3A) (17). While this mutant expression had no effect on the positive signaling Ptc-Smo-Gli in HCT8 or 3T3 cells (Suppl Fig 4 A, B) (17, 18, 35), we observed, using co-immunoprecipitation followed by immunoblot, that

PtcDN blocked Ptc/FHL-2 (Fig 3B) and Ptc/caspase-9 (Fig 3C) interactions. Moreover, we showed that the molecular complex containing Ptc and caspase-9 was modulated by the availability of SHH since the presence of rSHH induced the disruption of the Ptc-caspase-9 complex while this interaction was restored by the concomitant addition of the 5E1 SHH-blocking antibody (Fig 3D). Thus, PtcDN acts as an inhibitor of endogenous Ptc pro-apoptotic signaling by preventing Ptc dependosome complex formation (35). Reciprocally, a possible effect of endogenous Ptc on PtcDN is not excluded but unknown so far. We then analyzed the effect of PtcDN on Ptc-induced cell death triggered by SHH interference in HCT8 and LoVo cells. As expected, these cells expressing PtcDN (Fig 3E) failed to undergo apoptosis in comparison to control cells (peak-transfected cells) upon silencing of SHH by siRNA (Fig 3F and Suppl Fig 2D), or upon treatment with the 5E1 antibody (Fig 3G), both treatments having no effect on the positive signaling Ptc-Smo-Gli in HCT8 nor in other cell lines used in this study (Suppl Fig 4C, D). Together these results indicate that SHH expression in cancer cells inhibits Ptc pro-apoptotic activity and is likely implicated in the maintenance of HCT8 and LoVo cells survival.

Disruption of SHH autocrine loop triggers tumor growth inhibition *in vivo* through Ptc-induced cell death

We next challenged the hypothesis that interfering with SHH autocrine loop could trigger *in vivo* tumor growth inhibition. First, we used an avian model that recapitulates tumor progression and dissemination. Grafts of tumor cells in the chorioallantoic membrane (CAM) of 10-day-old chick embryos induce the growth of a primary tumor at the

implantation site - within the CAM- as well as metastasis dissemination at distant sites – e.g. in the lung (Fig 4A) (40). CAMs in 10-day-old fertilized chicken eggs were inoculated either with mock transfected HCT8 (HCT8 peak) or HCT8 expressing PtcDN (HCT8 PtcDN) cells and were treated on day 11 and day 14 with either isotype control IgG or 5E1 blocking antibody. Three days later, primary tumor volumes were measured and the lungs were removed from the embryos and analyzed for the presence of metastasis. As shown in Figure 4B, C, D, treatment of CAM-grafted HCT8 cells with the 5E1 antibody reduced significantly the size of primary tumors and decreased the incidence of lung metastasis development. In contrast, the 5E1 antibody had no effect on either primary tumor growth nor metastasis dissemination in eggs grafted with HCT8 PtcDN cells (Fig 4 B, C, D).

In order to confirm these results in another *in vivo* metastatic model, we used a zebrafish model (41). We injected in the perivitelline space of 2-day-old zebrafish larvae HCT8 peak or PtcDN cells previously treated with isotype control IgG or 5E1 blocking antibody for 2 days and then stained with lyophilic DiO (green) and DiD dye (red), respectively. 48h after injection fishes were imaged and the number of metastatic cells in the tail was determined. As shown in Figure 4 E, F, treatment with the 5E1 antibody decreases significantly the number of metastatic HCT8 peak cells. In contrast, the 5E1 antibody had no effect on metastasis dissemination in fishes injected with HCT8 PtcDN cells (Fig 4E, F) supporting the view that interference with SHH decreases HCT8 cell dissemination mediated by Ptc.

To further define whether SHH interference is associated with an anti-tumor effect *in vivo*, we generated xenografts of SHH expressing tumor cells in nude mice. We

thus subcutaneously grafted HCT8 peak or HCT8 PtcDN cells in nude mice. When the tumors reached 70mm³, mice were treated intraperitoneally three times a week, with either SHH siRNA or with scrambled control siRNA as it has been successfully performed previously (32,38). We first showed that HCT8 tumors express SHH at transcriptional (Suppl Fig 5A) and protein level (Suppl Fig 5B) and, as shown in Suppl Fig 5C, treatment with SHH siRNA reduced significantly the growth of HCT8 peak tumors. In contrast, the siRNA had no effect on the growth of HCT8 PtcDN tumors (Suppl. Fig.5D). Alternative treatments were performed using the 5E1 SHH-blocking antibody. As shown in Figure 5A, B, 5E1 antibody treatment, which does not demonstrate apparent animal toxicity as attested by absence of weight variation during treatment (Suppl Fig 5E, F), significantly reduced the growth of HCT8 peak tumors (Fig 5A, B), a phenomenon associated with a significant reduction of the net tumor weight at the end of treatment protocol. In contrast, the growth of HCT8 PtcDN tumors (tumor volume as well as net tumor weight) was not affected by the treatment with the 5E1 antibody (Fig 5A, C, D). Similar results were obtained with LoVo-engrafted tumors (Suppl Fig 6A-C) confirming these results in another colon cell line. Of interest, 5E1 treatment triggered significant apoptosis -as measured by increased caspase-3 activity- in HCT8 peak but not in HCT8 PtcDN tumors (Fig 5E). Taken together these data support the view that SHH expression in cancer cells is associated with tumor growth and metastasis at least in part by inhibiting Ptc-induced cell death.

DISCUSSION

Here we have shown that colon, pancreatic and lung cancers that share the property to overexpress SHH also expresses Ptc-pro-apoptotic signaling effectors. Of prime importance, we also observed that disrupting the SHH autocrine loop, either by downregulating SHH expression or by blocking the interaction of SHH with Ptc, leads to tumor cell death *in vitro* and to a reduction of tumor growth and metastasis dissemination *in vivo*. These observations are in perfect agreement with the fact that Ptc belongs to the family of dependence receptors (17,42) that have been proposed to act as a safeguard mechanism against tumor progression (28,43,44). Reciprocally, the overexpression of dependence receptor ligand is also known to confer a selective advantage on tumor cell survival by blocking dependence receptor-mediated cell death. Along this line, it has been shown that netrin-1, the ligand of DCC/UNC5 family, is a promising therapeutic target in netrin-1-overexpressing tumors (32,38) leading to ongoing clinical trial investigating whether inhibition of netrin-1 activity could be effective in solid human tumors (<https://clinicaltrials.gov/ct2/show/NCT02977195>). Similarly, NT3 the ligand of TrkC dependence receptor is also promoting tumor cell survival in neuroblastoma (33) as well as Sema3E which blocks the cell death induced by Plexin D1 in breast cancer (45).

Given that a high proportion of cancer pathologies show aberrant Hedgehog signaling, many antagonist molecules of this signaling pathway with putative therapeutic activity have been developed these last fifteen years. Most of these drugs target the canonical pathway -i.e., Ptc-Smo-Gli components of the pathway-. In that regard, the Smo antagonists Vismodegib and Sonidegib has demonstrated anti-tumor effects in basal cell carcinoma (BCC) and medulloblastoma bearing activated somatic mutations

(46,47) and is approved for treating BCC. Nevertheless, Vismodegib failed to show any beneficial effect in phase II clinical trial including patients with tumors with HH up-regulation such as colorectal, ovarian cancer and chondrosarcoma. The study we present here allows to propose that the lack of clinical effect of these "canonical pathway" inhibitors is probably a consequence of their inability to promote Ptc-induced apoptosis. Such apoptotic stimulation would be highly interesting to be tested in colon and pancreatic cancers in which respectively 80% and 64% of the tumors overexpress SHH. In the case of lung tumors, the situation is a little bit more uncertain since in spite of expressing all the effectors of Ptc-induced cell death pathway only 8% of them overexpress SHH. Nevertheless, HH pathway has been proposed to be involved in resistance to radiotherapy and to immune checkpoint inhibitors and relapse in lung cancer (48), even though resistance mechanisms are still poorly understood. Hence, future work will have to investigate whether targeting SHH/Ptc interaction in these tumors may turn as a promising therapeutic strategy.

Concerning CDON, another SHH receptor previously described as a dependence receptor frequently lost in cancers (18), it is expressed, at least at the mRNA level, in SHH-expressing colon, pancreatic and NSCLC cancers (18). Similarly, in the selected HCT8 cell line used in this study, CDON expression was detected at mRNA level but we failed to detect its expression at the protein level. Moreover, we did not observe a putative involvement of CDO-proapoptotic signaling upon SHH withdrawal.

Future studies aimed at defining therapeutic approaches will probably be based on antibodies that block the interaction between SHH and either Ptc and CDON unleashing Ptc or/and CDON-induced cell death. Interestingly, based on the predicted

interacting structures of SHH with Ptc or CDON (49), SHH antibodies such as 5E1 should interfere with both interactions. Another point to investigate concerns the not yet fully elucidated pathways of CDON- and Ptc-induced cell death. So far, it seems that downstream effectors involved in both pathways are different since, for example, the dependosome complex does not appear recruited by CDON. Also, it is still not known whether some interaction/synergy between both pathways occurs.

Future works will also have to investigate whether a therapeutic approach targeting SHH/Ptc interaction would be efficient on both tumor and stroma cell death. It has indeed been suggested that autocrine and paracrine SHH signaling cooperate in some tumors (50). For example, in colon, pancreatic and ovarian cancers, SHH ligand secreted from epithelial tumor cells has been shown to activate SHH signaling in the tumor-associated stromal tissues, which, in turn, could provide a more favorable environment for tumor development. We can thus speculate that targeting SHH ligand could also trigger Ptc-induced cell death in stromal cells and, as an indirect consequence, also prevent tumor progression, even though at this stage we do not know whether, upon paracrine expression of SHH, stromal cells are prime to be dependent for survival on SHH. Together, our work and the different preclinical data showing robust anti-tumor activity of anti-SHH antibodies (15,16) strengthen the view that, even though the pharmaceutical industry is current moving away from the HH field, it would actually be of key interest to clinically investigate the efficiency of SHH antibodies compared to HH canonical pathway inhibitors in SHH-overexpressing tumors and to eventually consider it in combination with other current anti-tumor therapies.

ACKNOWLEDGEMENTS:

We wish to thank Emilie Servoz (from LMT) for technical assistance in the animal facility. This work was supported by institutional grants from CNRS, University of Lyon, Centre Léon Bérard and from the Ligue Contre le Cancer, INCA, ANR and ERC. Pauline Mathot has been supported by a fellowship from la Ligue Contre le Cancer. Sachitanand M. Mali and Rudi Fasan acknowledge support from the U.S. National Institute of Health grant R01 GM134076.

REFERENCES

1. Jessell TM. Neuronal specification in the spinal cord: inductive signals and transcriptional codes. *Nat Rev Genet.* **2000**;1:20–9.
2. Ingham PW, McMahon AP. Hedgehog signaling in animal development: paradigms and principles. *Genes Dev.* **2001**;15:3059–87.
3. Beachy PA, Karhadkar SS, Berman DM. Tissue repair and stem cell renewal in carcinogenesis. *Nature.* **2004**;432:324–31.
4. Pasca di Magliano M, Hebrok M. Hedgehog signalling in cancer formation and maintenance. *Nat Rev Cancer.* **2003**;3:903–11.
5. Dahmane N, Lee J, Robins P, Heller P, Ruiz i Altaba A. Activation of the transcription factor Gli1 and the Sonic hedgehog signalling pathway in skin tumours. *Nature.* **1997**;389:876–81.
6. Watkins DN, Berman DM, Burkholder SG, Wang B, Beachy PA, Baylin SB. Hedgehog signalling within airway epithelial progenitors and in small-cell lung cancer. *Nature.* **2003**;422:313–7.
7. Berman DM, Karhadkar SS, Maitra A, Montes De Oca R, Gerstenblith MR, Briggs K, et al. Widespread requirement for Hedgehog ligand stimulation in growth of digestive tract tumours. *Nature.* **2003**;425:846–51.
8. Thayer SP, di Magliano MP, Heiser PW, Nielsen CM, Roberts DJ, Lauwers GY, et al. Hedgehog is an early and late mediator of pancreatic cancer tumorigenesis. *Nature.* **2003**;425:851–6.

9. Raffel C, Jenkins RB, Frederick L, Hebrink D, Alderete B, Fults DW, et al. Sporadic medulloblastomas contain PTCH mutations. *Cancer Res.* **1997**;57:842–5.
10. Taylor MD, Liu L, Raffel C, Hui C, Mainprize TG, Zhang X, et al. Mutations in SUFU predispose to medulloblastoma. *Nat Genet.* **2002**;31:306–10.
11. Yauch RL, Gould SE, Scales SJ, Tang T, Tian H, Ahn CP, et al. A paracrine requirement for hedgehog signalling in cancer. *Nature.* **2008**;455:406–10.
12. Rimkus TK, Carpenter RL, Qasem S, Chan M, Lo H-W. Targeting the Sonic Hedgehog Signaling Pathway: Review of Smoothed and GLI Inhibitors. *Cancers (Basel).* **2016**;8.
13. Scales SJ, de Sauvage FJ. Mechanisms of Hedgehog pathway activation in cancer and implications for therapy. *Trends Pharmacol Sci.* **2009**;30:303–12.
14. Tremblay MR, Nesler M, Weatherhead R, Castro AC. Recent patents for Hedgehog pathway inhibitors for the treatment of malignancy. *Expert Opin Ther Pat.* **2009**;19:1039–56.
15. Coon V, Laukert T, Pedone CA, Laterra J, Kim KJ, Fults DW. Molecular therapy targeting Sonic hedgehog and hepatocyte growth factor signaling in a mouse model of medulloblastoma. *Mol Cancer Ther.* **2010**;9:2627–36.
16. Chang Q, Foltz WD, Chaudary N, Hill RP, Hedley DW. Tumor-stroma interaction in orthotopic primary pancreatic cancer xenografts during hedgehog pathway inhibition. *Int J Cancer.* **2013**;133:225–34.
17. Thibert C, Teillet M-A, Lapointe F, Mazelin L, Le Douarin NM, Mehlen P. Inhibition of neuroepithelial patched-induced apoptosis by sonic hedgehog. *Science.* **2003**;301:843–6.
18. Delloye-Bourgeois C, Gibert B, Rama N, Delcros J-G, Gadot N, Scoazec J-Y, et al. Sonic Hedgehog promotes tumor cell survival by inhibiting CDON pro-apoptotic activity. *PLoS Biol.* **2013**;11:e1001623.
19. Mehlen P, Rabizadeh S, Snipas SJ, Assa-Munt N, Salvesen GS, Bredesen DE. The DCC gene product induces apoptosis by a mechanism requiring receptor proteolysis. *Nature.* **1998**;395:801–4.
20. Mehlen P, Thibert C. Dependence receptors: between life and death. *Cell Mol Life Sci.* **2004**;61:1854–66.
21. Matsunaga E, Tauszig-Delamasure S, Monnier PP, Mueller BK, Strittmatter SM, Mehlen P, et al. RGM and its receptor neogenin regulate neuronal survival. *Nat Cell Biol.* **2004**;6:749–55.

22. Bordeaux MC, Forcet C, Granger L, Corset V, Bidaud C, Billaud M, et al. The RET proto-oncogene induces apoptosis: a novel mechanism for Hirschsprung disease. *EMBO J*. **2000**;19:4056–63.
23. Lin S, Negulescu A, Bulusu S, Gibert B, Delcros J-G, Ducarouge B, et al. Non-canonical NOTCH3 signalling limits tumour angiogenesis. *Nat Commun*. **2017**;8:16074.
24. Wang H, Boussouar A, Mazelin L, Tauszig-Delamasure S, Sun Y, Goldschneider D, et al. The Proto-oncogene c-Kit Inhibits Tumor Growth by Behaving as a Dependence Receptor. *Mol Cell*. **2018**;72:413-425.e5.
25. Mehlen P, Bredesen DE. The dependence receptor hypothesis. *Apoptosis*. **2004**;9:37–49.
26. Furne C, Rama N, Corset V, Chédotal A, Mehlen P. Netrin-1 is a survival factor during commissural neuron navigation. *Proc Natl Acad Sci USA*. **2008**;105:14465–70.
27. Mourali J, Bénard A, Lourenço FC, Monnet C, Greenland C, Moog-Lutz C, et al. Anaplastic lymphoma kinase is a dependence receptor whose proapoptotic functions are activated by caspase cleavage. *Mol Cell Biol*. **2006**;26:6209–22.
28. Mehlen P, Puisieux A. Metastasis: a question of life or death. *Nat Rev Cancer*. **2006**;6:449–58.
29. Grady WM. Making the case for DCC and UNC5C as tumor-suppressor genes in the colon. *Gastroenterology*. **2007**;133:2045–9.
30. Castets M, Broutier L, Molin Y, Brevet M, Chazot G, Gadot N, et al. DCC constrains tumour progression via its dependence receptor activity. *Nature*. **2011**;482:534–7.
31. Fitamant J, Guenebeaud C, Coissieux M-M, Guix C, Treilleux I, Scoazec J-Y, et al. Netrin-1 expression confers a selective advantage for tumor cell survival in metastatic breast cancer. *Proc Natl Acad Sci USA*. **2008**;105:4850–5.
32. Delloye-Bourgeois C, Fitamant J, Paradisi A, Cappellen D, Douc-Rasy S, Raquin M-A, et al. Netrin-1 acts as a survival factor for aggressive neuroblastoma. *J Exp Med*. **2009**;206:833–47.
33. Bouzas-Rodriguez J, Cabrera JR, Delloye-Bourgeois C, Ichim G, Delcros J-G, Raquin M-A, et al. Neurotrophin-3 production promotes human neuroblastoma cell survival by inhibiting TrkC-induced apoptosis. *J Clin Invest*. **2010**;120:850–8.
34. Paradisi A, Maise C, Coissieux M-M, Gadot N, Lépinasse F, Delloye-Bourgeois C, et al. Netrin-1 up-regulation in inflammatory bowel diseases is required for colorectal cancer progression. *Proc Natl Acad Sci USA*. **2009**;106:17146–51.

35. Mille F, Thibert C, Fombonne J, Rama N, Guix C, Hayashi H, et al. The Patched dependence receptor triggers apoptosis through a DRAL-caspase-9 complex. *Nat Cell Biol.* **2009**;11:739–46.
36. Wan Y-W, Allen GI, Liu Z. TCGA2STAT: simple TCGA data access for integrated statistical analysis in R. *Bioinformatics.* **2016**;32:952–4.
37. Owens AE, de Paola I, Hansen WA, Liu Y-W, Khare SD, Fasan R. Design and Evolution of a Macrocyclic Peptide Inhibitor of the Sonic Hedgehog/Patched Interaction. *J Am Chem Soc.* **2017**;139:12559–68.
38. Delloye-Bourgeois C, Brambilla E, Coissieux M-M, Guenebeaud C, Pedeux R, Firlej V, et al. Interference with netrin-1 and tumor cell death in non-small cell lung cancer. *J Natl Cancer Inst.* **2009**;101:237–47.
39. Douard R, Moutereau S, Pernet P, Chimingqi M, Allory Y, Manivet P, et al. Sonic Hedgehog-dependent proliferation in a series of patients with colorectal cancer. *Surgery.* **2006**;139:665–70.
40. Stupack DG, Teitz T, Potter MD, Mikolon D, Houghton PJ, Kidd VJ, et al. Potentiation of neuroblastoma metastasis by loss of caspase-8. *Nature.* **2006**;439:95–9.
41. Teng Y, Xie X, Walker S, White DT, Mumm JS, Cowell JK. Evaluating human cancer cell metastasis in zebrafish. *BMC Cancer.* **2013**;13:453.
42. Fombonne J, Bissey P-A, Guix C, Sadoul R, Thibert C, Mehlen P. Patched dependence receptor triggers apoptosis through ubiquitination of caspase-9. *Proc Natl Acad Sci USA.* **2012**;109:10510–5.
43. Bernet A, Mehlen P. Dependence receptors: when apoptosis controls tumor progression. *Bull Cancer.* **2007**;94:E12-17.
44. Mazelin L, Bernet A, Bonod-Bidaud C, Pays L, Arnaud S, Gespach C, et al. Netrin-1 controls colorectal tumorigenesis by regulating apoptosis. *Nature.* **2004**;431:80–4.
45. Luchino J, Hocine M, Amoureux M-C, Gibert B, Bernet A, Royet A, et al. Semaphorin 3E suppresses tumor cell death triggered by the plexin D1 dependence receptor in metastatic breast cancers. *Cancer Cell.* **2013**;24:673–85.
46. Sekulic A, Migden MR, Oro AE, Dirix L, Lewis KD, Hainsworth JD, et al. Efficacy and safety of vismodegib in advanced basal-cell carcinoma. *N Engl J Med.* **2012**;366:2171–9.
47. Gajjar A, Stewart CF, Ellison DW, Kaste S, Kun LE, Packer RJ, et al. Phase I study of vismodegib in children with recurrent or refractory medulloblastoma: a pediatric brain tumor consortium study. *Clin Cancer Res.* **2013**;19:6305–12.

48. Giroux Leprieur E, Vieira T, Antoine M, Rozensztajn N, Rabbe N, Ruppert A-M, et al. Sonic Hedgehog Pathway Activation Is Associated With Resistance to Platinum-Based Chemotherapy in Advanced Non-Small-Cell Lung Carcinoma. *Clin Lung Cancer*. **2016**;17:301–8.
49. Beachy PA, Hymowitz SG, Lazarus RA, Leahy DJ, Siebold C. Interactions between Hedgehog proteins and their binding partners come into view. *Genes Dev*. **2010**;24:2001–12.
50. Theunissen J-W, de Sauvage FJ. Paracrine Hedgehog signaling in cancer. *Cancer Res*. **2009**;69:6007–10.

FIGURE LEGENDS

Figure 1: SHH-overexpressing tumors show expression of Ptc-proapoptotic signaling effectors

(A) Transcriptional expression level in RPKM of *SHH* in Colon Adenocarcinoma (n=283), Pancreatic Adenocarcinoma (n=178), and Non-Small Cell Lung (NSCL) Carcinoma (n=1016). Expression levels were analyzed in paired normal/tumoral samples from TCGA data base. **(B)** Percentage of SHH-upregulated tumors compared to normal tissues; SHH expression in tumors above twice the average value of SHH expression in normal tissues. **(C)** Representative SHH and Ptc immunohistochemistry on human colon and pancreatic adenocarcinoma. Bar: 100 μ M. **(D)** Transcriptional expression level of *PTCH1*, *CASP9*, *FHL2*, *CARD8*, *NLRP1*, and *NEDD4* genes in RPKM in Colon, Pancreatic and NSCL with SHH upregulation.

Figure 2: SHH inhibition triggers cell death *in vitro*

(A) SHH, Ptc, FHL2/DRAL and Caspase-9 (Casp-9) protein levels are analyzed by immunoblot in different representative cell lines from colon (HCT8, SW1417), pancreatic (Mia PaCa-2, Capan-2) and NSCLC (A549) cancers. b-actin is used as a loading control. **(B)** Expression of SHH at transcriptional level was measured by qRT-PCR, 24 hours after transfection with control siRNA (siRNA Ctrl) or SHH siRNA (siRNA SHH). **(C-D)** Caspase-3 activity was assessed 24h after (C) transfection with control siRNA (siRNA Ctrl) or SHH siRNA (siRNA SHH) (D) in the presence of 300ng/ml of recombinant SHH. **(E)** Ptc Cell death was analyzed by propidium iodide (PI) staining quantified by Incucyte Live cells analysis system. Number of PI positive cells normalized on the percentage of confluency are shown 72h after transfection with control siRNA (siCtrl), SHH siRNA (siSHH), Ptc siRNA (siPtc) or SHH and Ptc siRNAs (siSHH+siPtc). **(F)** mRNA expression analyzed by RT-qPCR in HCT8 cells 48h after transfection with control siRNA (siRNA Ctrl) or Ptc siRNA (siRNA Ptc). Errors bars are SEM. * : $p < 0.05$; ** : $p < 0.01$ calculated using two-sided Mann-Whitney test compared with level of control (siRNA Ctrl).

Figure 3: PtcDN expression disrupts apoptotic complex recruited by Ptc and inhibits cell death induced by SHH interference in HCT8 colon cells

(A) Schematic representation of the dominant negative mutant of Ptc (PtcDN) which is the seven intra-cellular domain mutated on the caspase cleavage site (D1392N). **(B-C)** HEK293T cells were co-transfected with Ptc expressing vector alone or with FLAG-Casp-9 or FLAG-FHL2/DRAL and in the presence or in the absence of HA-PtcDN expressing vector. (B) Ptc/FHL2 and (C) Ptc/Caspase-9 molecular complexes were

assessed by pull-down assay using α -FLAG antibody (IP: α -FLAG) followed by immunoblots of Ptc (WB: α -Ptc). Immunoblot on total lysates before pull-down are also displayed (Tot. prot.). **(D)** HEK293T cells were co-transfected with Ptc expressing vector alone or with FLAG-Casp-9. In presence of 300ng/ml recombinant SHH (lane Casp-9-FLAG+rSHH), Ptc binding to caspase-9 was decreased, while concomitant addition of the SHH-blocking 5E1 antibody (5 μ g/mL) (lane Casp-9-FLAG+rSHH+ 5E1 Ab) restored the interaction. Western blot on lysates before pull-down are shown (Tot. prot.). **(E)** Analysis of Ptc dominant negative (PtcDN) stably transfected in HCT8 cells by Western blot. PtcDN is expressed (lane PtcDN) in comparison to control cells transfected with peak8 empty vector (lane Peak). **(F-G)** Caspase-3 activity assays were performed in mock transfected control cells (HCT8 peak) and in stably transfected HCT8 cells with Ptc dominant negative (HCT8 PtcDN) (F) 24h after transfection with control siRNA (siRNA Ctrl) or SHH siRNA (siRNA SHH) or (G) after 24 h treatment with the SHH-neutralizing 5E1 monoclonal antibody (5E1 Ab - 5 μ g/mL) or an isotype control antibody (IgG Ctrl). Errors bars are SEM. * : $p < 0.05$; ** : $p < 0.01$ calculated using two-sided Mann-Whitney test compared with level of control.

Figure 4: SHH autocrine loop disruption reduces HCT8 tumor growth and metastasis dissemination in chick embryo chorioallantoic membrane (CAM) and zebrafish models

(A) Schematic representation of the experimental chick model. HCT8 cells were grafted in CAM at day 10. The SHH-neutralizing 5E1 antibody or an unrelated control IgG (10 μ g/ml) was injected in the tumors on day 11 and 13. Tumors and lungs were

harvested on day 17. **(B-D)** Effect of SHH-neutralizing antibody (5E1 Ab) on primary tumor growth and lung metastasis. **(B)** Representative images of primary tumors formed from control transfected cells (top) and PtcDN transfected cells (bottom) on CAM treated either with 5E1 antibody (right) or the unrelated control IgG (left). Bar: 2mm. **(C)** Quantitative analysis showing the mean of primary tumor size. **(D)** Percentage of embryos with lungs invaded by human HCT8 cells detected by qPCR on Alu sequences. **(E)** Representative images of 2dpf microinjected zebrafish in yolk sac with peak or PtcDN HCT8 cells. Cells were treated for 2 days with IgG isotype or 5E1 antibody (10 μ g/ml) then stained before injection with a lyophilic green DiO dye (IgG Ctrl) or red DiD dye (5E1 Ab). **(F)** Quantitative analysis of green and red metastatic cells. Results are from three independent experiments and are presented as mean \pm SEM. In C, ***: $p < 0.001$ calculated using Student t test compared with level of control (HCT8 peak IgG: $n=21$; 5E1 Ab: $n=18$ and HCT8 PtcDN PBS: $n=29$; 5E1 Ab: $n=29$). In D, *: $p < 0.05$ calculated using a Chi-squared test; (HCT8 peak IgG: $n=29$; 5E1 Ab: $n=29$ and HCT8 PtcDN PBS: $n=37$; 5E1 Ab: $n=38$). In F, : $p < 0.05$ calculated using Student t test compared with level of control (HCT8 peak IgG : $n=10$; 5E1 Ab: $n=11$ and HCT8 PtcDN PBS: $n=10$; 5E1 Ab: $n=10$).

Figure 5: SHH autocrine loop disruption constrains HCT8 tumor growth through Ptc-induced cell death in nude mice model

(A) Representative image of tumor from HCT8 peak and HCT8 PtcDN engrafted mice after control buffer (PBS) or 5E1 treatment (5E1 Ab). **(B-C)** Effect of the SHH-neutralizing antibody on HCT8 xenograft tumor growth in mice and on intra-tumoral

apoptosis. Volume of tumors derived from (B) control (HCT8 peak) or (C) PtcDN HCT8 cells were measured during 21 days. Intra-tumoral injections of either 5E1 antibody (5E1 Ab – 300µg) or control buffer (PBS) were performed 3 times a week. Mean tumor volume is indicated. **(D)** The weight of tumors derived from control or ptcDN transfected HCT8 cells was analyzed after 21 days of treatment with 5E1 antibody or control buffer. **(E)** Quantification of caspase-3 activity in xenograft lysates analyzed after 2 days of intra-tumoral treatment. In A and B, results are presented as mean +/- SEM (HCT8 peak PBS :n=10 ; 5E1 Ab: n=9 and HCT8 PtcDN PBS: n=9; 5E1 Ab: n=9). p value or NS (not significant) is obtained using two-way ANOVA statistical test. Errors bars are SEM. * : p<0.05 ; *** : p<0.001 calculated using Student t test compared with level of control (PBS).

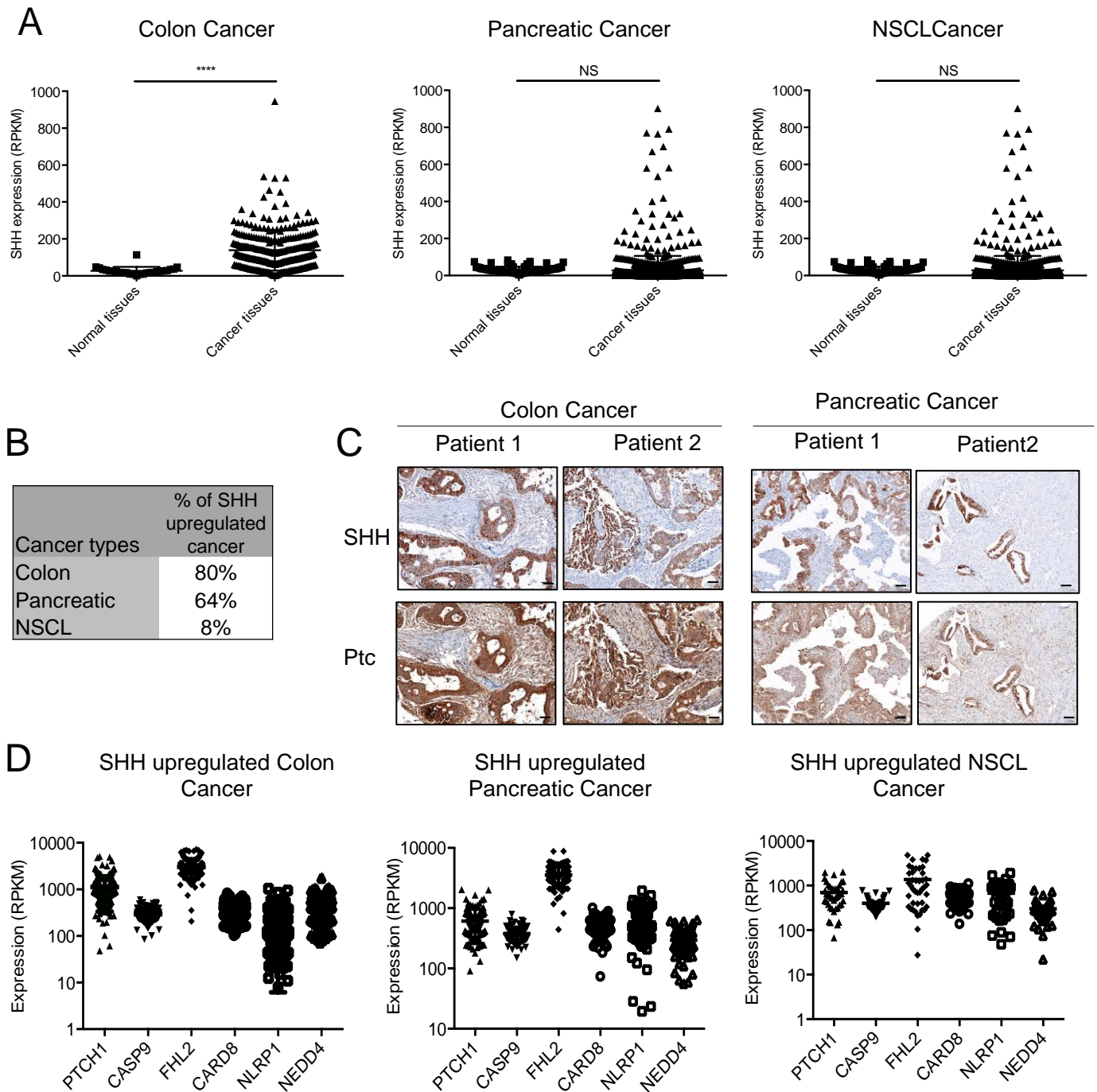


Figure 2

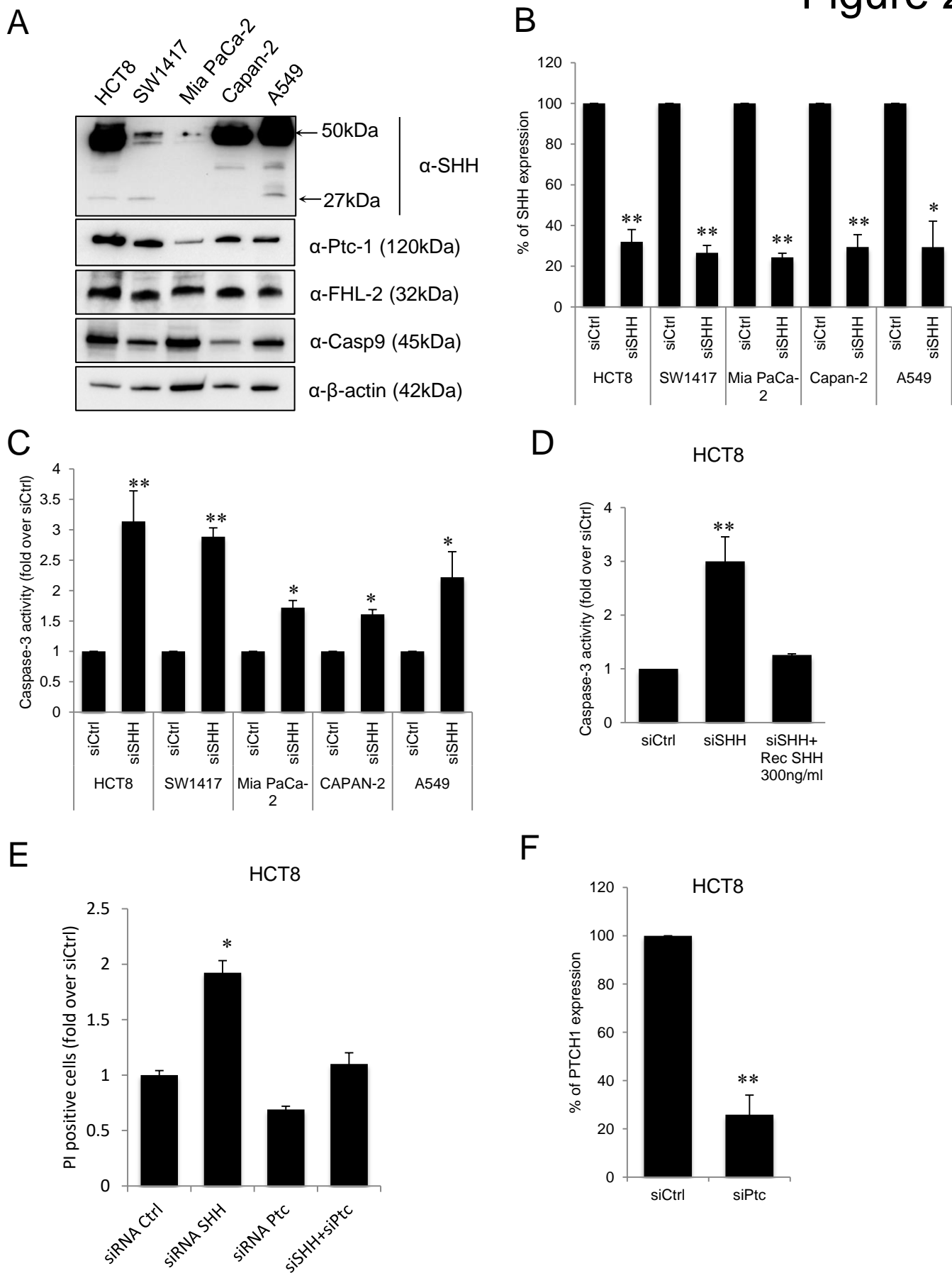
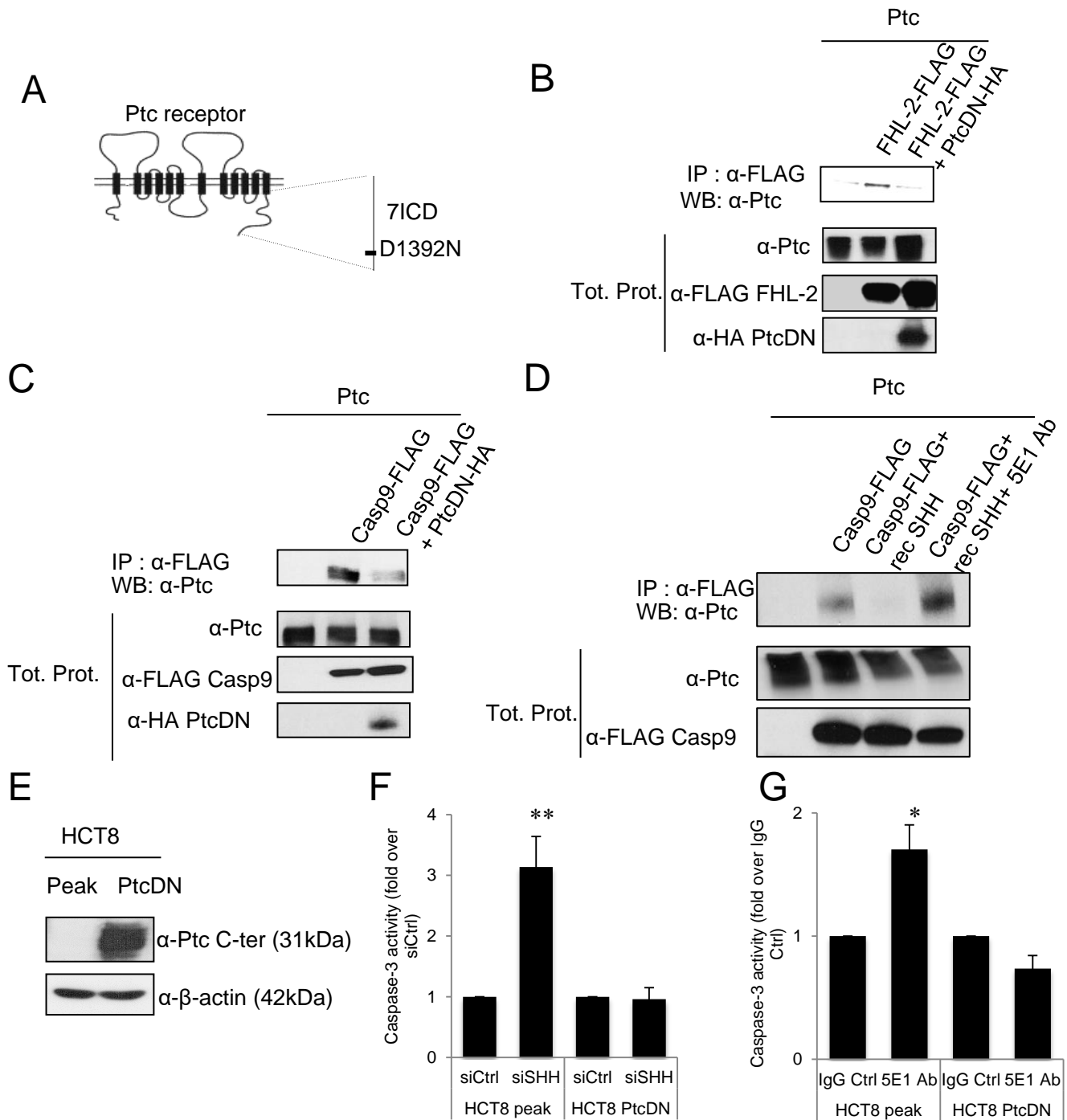
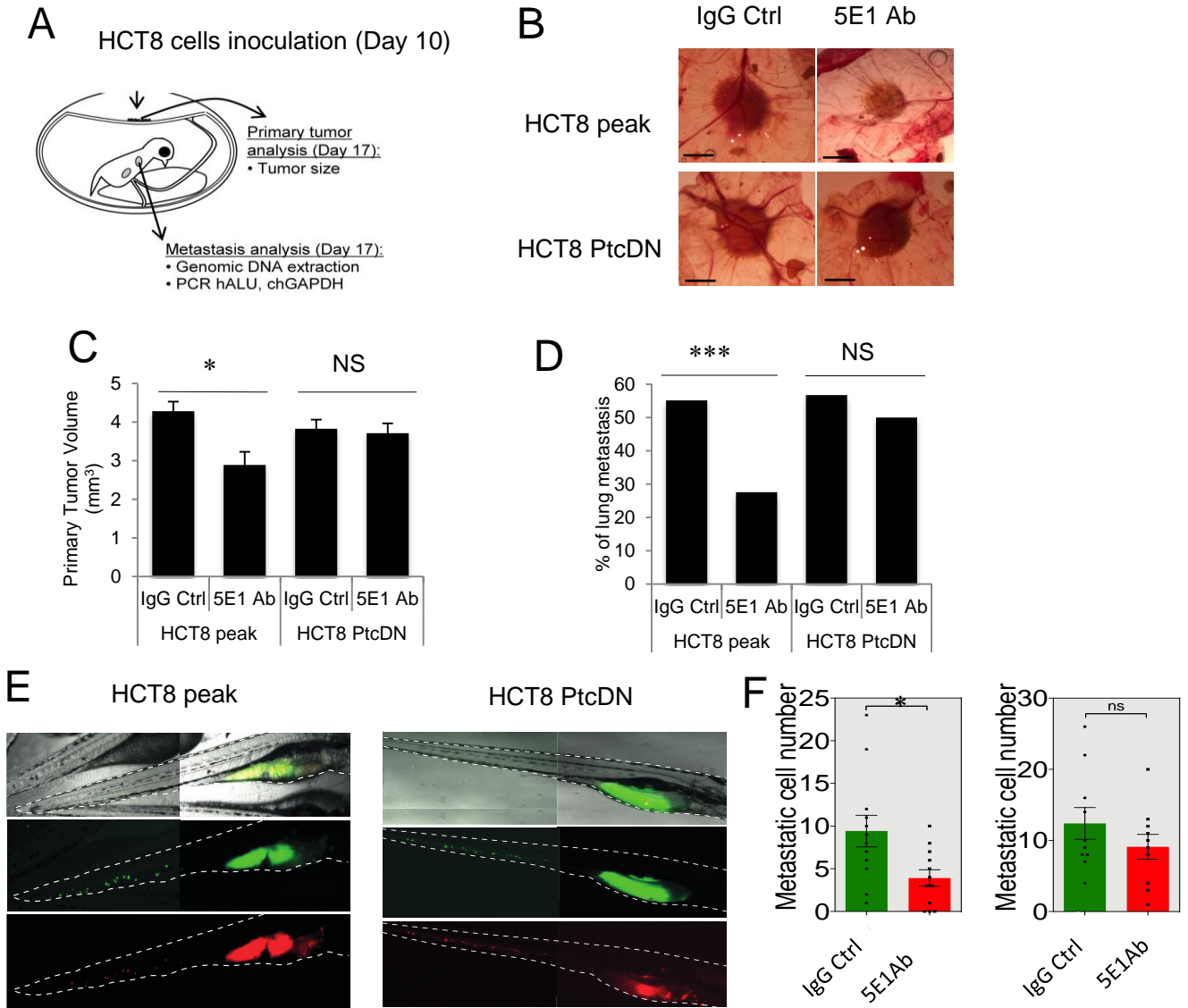
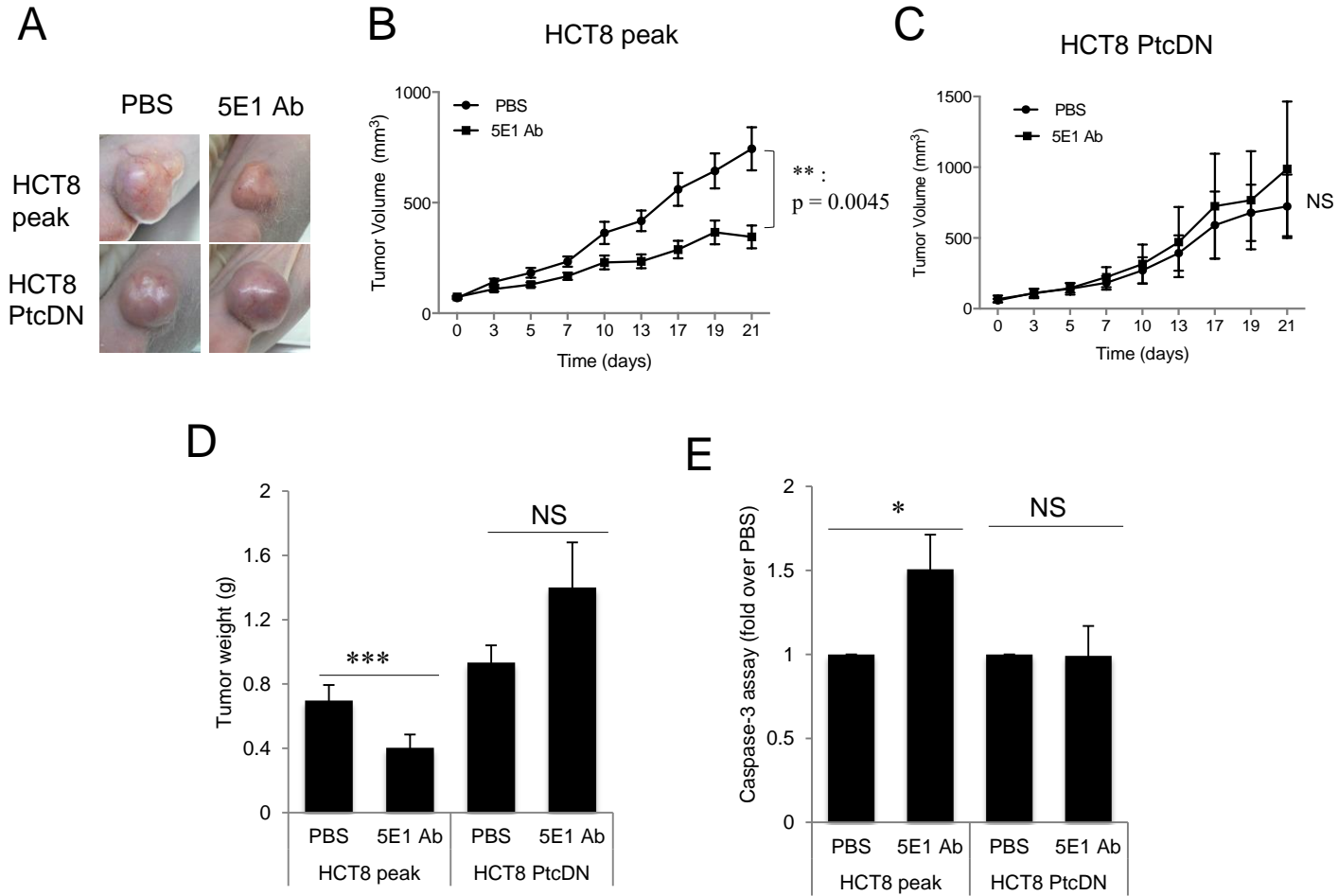


Figure 3







Cancer Research

The Journal of Cancer Research (1916–1930) | The American Journal of Cancer (1931–1940)

Blocking SHH/Patched interaction triggers tumor growth inhibition through Patched-induced apoptosis

Pierre-Antoine Bissey, Pauline Mathot, Catherine Guix, et al.

Cancer Res Published OnlineFirst February 14, 2020.

Updated version	Access the most recent version of this article at: doi: 10.1158/0008-5472.CAN-19-1340
Supplementary Material	Access the most recent supplemental material at: http://cancerres.aacrjournals.org/content/suppl/2020/02/14/0008-5472.CAN-19-1340.DC1
Author Manuscript	Author manuscripts have been peer reviewed and accepted for publication but have not yet been edited.

E-mail alerts [Sign up to receive free email-alerts](#) related to this article or journal.

Reprints and Subscriptions To order reprints of this article or to subscribe to the journal, contact the AACR Publications Department at pubs@aacr.org.

Permissions To request permission to re-use all or part of this article, use this link <http://cancerres.aacrjournals.org/content/early/2020/02/14/0008-5472.CAN-19-1340>. Click on "Request Permissions" which will take you to the Copyright Clearance Center's (CCC) Rightslink site.